Roles of key active-site residues in flavocytochrome P450 BM3

Michael A. NOBLE*, Caroline S. MILES*, Stephen K. CHAPMAN*, Dominikus A. LYSEK*, Angela C. MACKAY*, Graeme A. REID†, Robert P. HANZLIK‡ and Andrew W. MUNRO*[1]

*Department of Chemistry, University of Edinburgh, The King's Buildings, West Mains Road, Edinburgh EH9 3JJ, U.K., †Institute of Cell and Molecular Biology, University of Edinburgh, Edinburgh EH9 3JR, U.K., and ‡Department of Medicinal Chemistry, University of Kansas, Lawrence, KS 66045, U.S.A.

The effects of mutation of key active-site residues (Arg-47, Tyr-51, Phe-42 and Phe-87) in *Bacillus megaterium* flavocytochrome P450 BM3 were investigated. Kinetic studies on the oxidation of laurate and arachidonate showed that the side chain of Arg-47 contributes more significantly to stabilization of the fatty acid carboxylate than does that of Tyr-51 (kinetic parameters for oxidation of laurate: R47A mutant, K_m 859 μM, k_{cat} 3960 min^{-1}; Y51F mutant, K_m 432 μM, k_{cat} 6140 min^{-1}; wild-type, K_m 288 μM, k_{cat} 5140 min^{-1}). A slightly increased k_{cat} for the Y51F-catalysed oxidation of laurate is probably due to decreased activation energy ($\Delta G^{\ddagger}$) resulting from a smaller ΔG of substrate binding. The side chain of Phe-42 acts as a phenyl 'cap' over the mouth of the substrate-binding channel. With mutant F42A, K_m is massively increased and k_{cat} is decreased for oxidation of both laurate (K_m 2.08 mM, k_{cat} 2450 min^{-1}) and arachidonate (K_m 34.9 μM, k_{cat} 14620 min^{-1}; compared with values of 4.7 μM and 17100 min^{-1} respectively for wild-type). Amino acid Phe-87 is critical for efficient catalysis. Mutants F87G and F87Y not only exhibit increased K_m and decreased k_{cat} values for fatty acid oxidation, but also undergo an irreversible conversion process from a 'fast' to a 'slow' rate of substrate turnover [for F87G (F87Y)-catalysed laurate oxidation: k_{cat} 'fast', 760 (1620) min^{-1}; k_{cat} 'slow', 48.0 (44.6) min^{-1}; k_{conv} (rate of conversion from fast to slow form), 4.9 (23.8) min^{-1}]. All mutants showed less than 10% uncoupling of NADPH oxidation from fatty acid oxidation. The rate of FMN-to-haem electron transfer was shown to become rate-limiting in all mutants analysed. For wild-type P450 BM3, the rate of FMN-to-haem electron transfer (8340 min^{-1}) is twice the steady-state rate of oxidation (4100 min^{-1}), indicating that other steps contribute to rate limitation. Active-site structures of the mutants were probed with the inhibitors 12-(imidazolyl) dodecanoic acid and 1-phenylimidazole. Mutant F87G binds 1-phenylimidazole > 10-fold more tightly than does the wild-type, whereas mutant Y51F binds the haem-co-ordinating fatty acid analogue 12-(imidazolyl)dodecanoic acid > 30-fold more tightly than wild-type.

Key words: inhibition, kinetics, mutagenesis.

INTRODUCTION

The cytochromes *P*-450 (P450s) are a superfamily of haem enzymes that are involved in an enormous array of oxidative functions. They are found in organisms from all of the domains of life [1,2], and multiple forms exist in eukaryotes [3]. The eukaryotic forms are involved in several roles, including the synthesis and interconversions of steroids, and the production of prostaglandins and related eicosanoids [4]. Importantly, mammalian hepatic P450s play vital roles in the oxidation of drugs and exogenous toxins, facilitating the excretion of the more polar oxidized derivatives or targeting these molecules for subsequent metabolism by 'phase II' enzymes, such as glutathione S-transferases or UDP-glucuronyltransferases [5]. Generally, fewer P450s are found in lower eukaryotes and bacteria, although the recent determination of the entire genome sequence of *Mycobacterium tuberculosis* indicated the presence of 21 P450 and P450-like proteins [6]. In bacteria, the P450s have frequently evolved to catalyse the oxidation of environmental organic compounds, such as camphor, alkoxyphenols and herbicides, allowing these materials to be used as growth substrates [2,7,8].

The bacterial P450s are soluble enzymes, whereas their eukaryotic counterparts are generally integral membrane proteins, as are their reductase systems. The relative ease of overexpression, purification and crystallization of the bacterial forms has led to the solution of the structures of six P450s to date [2,9,10]. For two of these [the *Pseudomonas putida* camphor hydroxylase P450cam (CYP 101) and the *Bacillus megaterium* fatty acid hydroxylase P450 BM3 (CYP 102A1)], the structures of both substrate-bound and -free forms have been solved [11,12]. These structures provide templates for modelling eukaryotic P450s, and provide the basis for rational site-directed mutagenesis studies aimed at the elucidation of the roles of residues within the active site [13,14] and others that are retained across different branches of the P450 superfamily [15–17].

Arguably the most important model P450 is P450 BM3, a high-activity fatty acid hydroxylase in which the P450 is fused to its redox partner (a eukaryotic-like FAD- and FMN-containing NADPH–P450 reductase) in a single polypeptide [18,19]. The arrangement is analogous to that seen in the eukaryotic nitric oxide synthases [20]. P450 BM3 hydroxylates a large range of $\sim C_{12}$–C_{20} saturated and unsaturated fatty acids of carbon chain length. It is the fastest P450 mono-oxygenase known, with rates of over 5000 min^{-1} for the best substrates (e.g. arachidonic acid) [21]. The crystal structures of the substrate-free [11] and substrate (palmitoleate)-bound [12] forms have allowed the identification of a number of active-site residues likely to interact with substrate or to be otherwise involved in the catalytic process. These include: Arg-47 and Tyr-51, both of which are thought to interact with the carboxylate group of fatty acid substrates [12,14]; Phe-87, which is known to undergo a dramatic movement on substrate binding and to be vital in the control of the regiospecificity of substrate oxidation [22,23]; and Phe-42, which is located at the mouth of the long, hydrophobic fatty-acid-

Abbreviations used: P450, cytochrome P450 mono-oxygenase; ImC12, 12-(imidazolyl)dodecanoic acid; 1-PIM, 1-phenylimidazole.

[1] To whom correspondence should be addressed (e-mail Andrew.Munro@ed.ac.uk).

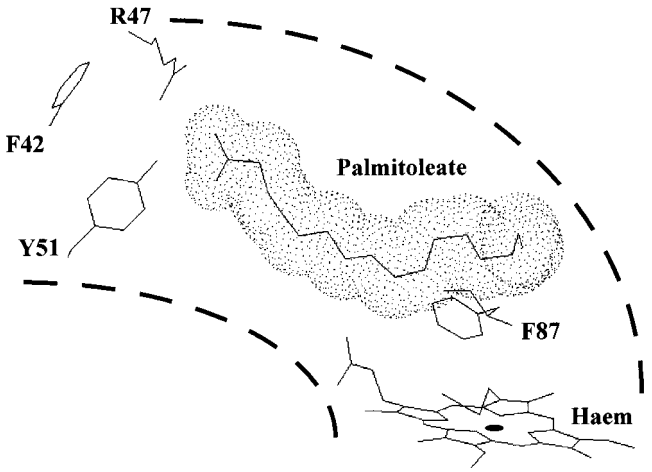

Figure 1 Schematic representation of the relative positions of residues Arg-47, Tyr-51, Phe-42 and Phe-87 in the active site of substrate (palmitoleate)-bound P450 BM3

Residues Arg-47, Tyr-51 and Phe-42 are located at the 'mouth' of the hydrophobic channel. Arg-47 and Tyr-51 offer potential interactions with the carboxy group of the fatty acid, and Phe-42 'caps' the active site. Phe-87 lies above the haem ring and interacts with the ω-terminus of fatty acid substrates. The dots around the palmitoleate indicate its van der Waals surface.

binding pocket of the P450, and which places a phenyl 'cap' over the mouth of the active site (Figure 1).

In the present paper, we report the catalytic properties and active-site structures of site-directed mutants of these key residues using steady-state and stopped-flow enzyme kinetics, and by spectrophotometric determinations of the affinities of binding of fatty acids and imidazole inhibitors. These studies have allowed us to evaluate the relative contributions of these residues to the catalytic process of P450 BM3, and to form a clearer picture of the mechanisms by which P450 BM3 regulates fatty acid oxidase function.

EXPERIMENTAL

Materials

All P450 BM3 substrates and other reagents were purchased from Sigma, and were of the highest grade available. The fatty acids used were sodium laurate and arachidonic acid. Sodium laurate (1 mM) was prepared in assay buffer (20 mM Mops/100 mM KCl, pH 7.4), which was used throughout for kinetic and binding studies. Arachidonic acid (33 mM or 3.3 mM) was prepared in methanol/ethanol (1:1, v/v). NADPH (20 mM) was prepared in ice-cold assay buffer. 12-(Imidazolyl)dodecanoic acid (ImC12) was synthesized and purified as described previously [24], and stock solutions (25–60 mM) were prepared in DMSO/methanol (1:1, v/v). 1-Phenylimidazole (1-PIM) was from Sigma, and stocks (10 mM and 100 mM) were prepared in ethanol/methanol (1:1, v/v). Cytochrome *c* (horse heart; type I) was from Sigma.

Escherichia coli strains and plasmid vectors

E. coli strain TG1 [*sup*E, *hsd*Δ5, *thi*, Δ(*lac-pro*AB), F′ (*tra*D36, *pro*AB$^+$, *lac*I^q, *lac*ZΔM15)] was used for all cloning work and for overexpression of intact P450 BM3. The preparation of the construct for the overexpression of intact P450 BM3 (plasmid pBM23, also referred to previously as pJM23) has been described in previous publications [19,25]. Plasmid clones encoding the active-site mutants R47G, F87G and F87Y of P450 BM3 were obtained from Dr. David Mullin and Professor William Alworth (Department of Chemistry, Tulane University, New Orleans, LA, U.S.A.) and overexpressed under a T7 promoter system from plasmid vector pTZ18U in strain BL21 (DE3) [*hsd*S, *gal* (λ*c*I*ts*857, *ind*1, Sam7, *nin*5, *lac*UV5-T7 gene 1)]. Mutants R47A, Y51F and F42A were created by oligonucleotide-directed mutagenesis of the pBM23 clone using the Kunkel method [26,27]. Single-stranded DNA was prepared using the helper phage M13 KO7 [28]. Oligonucleotide primers used in the mutagenesis procedure were as follows (mismatches indicated by the underlined bases): R47A, 5′ GTAGCGCGTTACAGCACCAGGCGCCTCG 3′; Y51F, 5′ GACTTGATAAGAAGCGCGTTAC 3′; F42A, 5′ CCAGGCGCCTCGGCTTTAAAGATTTCTCC 3′. Mutants were overexpressed in strain TG1 in identical fashion to the wild-type clone [25].

Enzyme preparations

Wild-type and mutant P450 BM3 enzymes were purified from *E. coli* transformants in strains BL21 (DE3) (R47G, F87Y and F87G) and TG1 (wild-type, R47A, Y51F and F42A) by growth of the BL21 (DE3) transformant cultures (2–5 litres in Luria–Bertani medium; 37 °C; shaking at 250 rev./min) for 6–12 h after induction at $A_{600} = 1$ with 500 μg/ml isopropyl β-D-thiogalactopyranoside, or by growth of the TG1 transformant cultures (which express the P450 to high levels from the *Bacillus* promoter in the stationary phase) for ~6 h after entry into stationary phase. Wild-type P450 BM3 and mutant forms were purified by column chromatography on DEAE-Sephacel and hydroxyapatite, as described previously [19,25]. A final gel-filtration step (Sephacryl S-200HR) was used to remove minor contaminating protein species. PMSF (1 mM) and leupeptin (1 mM) were added to all buffers to minimize proteolysis. All proteins were stored at −20 °C after two rounds of dialysis into successive 500-fold volumes of buffer A (50 mM Tris/HCl, pH 7.5) containing 50% (v/v) glycerol and protease inhibitors, and were used within 1 month of manufacture.

Spectrophotometric titrations of fatty acid substrate and inhibitor binding

UV/visible absorption spectra were recorded over 300–800 nm using a Shimadzu 2101 spectrophotometer and quartz cuvettes of 1 cm path-length. Typically the concentration of wild-type or mutant P450 BM3 used was 1–5 μM in 1 ml of assay buffer at 30 °C. For the titration of Y51F with ImC12, a much lower enzyme concentration was required, due to the very high affinity for the inhibitor (≈0.1 μM P450 used), and consequently a 5 cm-path-length cuvette was used. All spectral titrations were performed at 30 °C. For enzyme titrations with sodium laurate, 10 μl aliquots of a 2 μM solution of P450 BM3 in assay buffer were withdrawn and replaced with aliquots of a solution of enzyme at identical concentration in the same buffer, but containing in addition 1 mM sodium laurate. For the titrations to determine the binding of arachidonic acid, ImC12 and 1-PIM, small aliquots (0.1–0.4 μl; less than 5 μl total addition) of stock solution were added. Spectra were recorded after each addition of substrate or inhibitor. Difference spectra were generated by subtraction of each spectrum recorded from the original substrate- or inhibitor-free spectrum. K_d values were determined by plotting the maximal absorbance changes calculated from each difference spectrum against the concentration of substrate/imidazole and fitting the data to a rectangular hyperbola using Origin software (Microcal).

Kinetic measurements

All steady-state kinetic experiments were performed at 30 °C in assay buffer in 1 cm-path-length quartz cuvettes. Stopped-flow experiments were performed using an Applied Photophysics SF.17MV spectrophotometer.

Fatty acid oxidation

Fatty acid oxidation was determined as described previously [29]. Initial rates of fatty acid (arachidonate, laurate) oxidation were measured by monitoring the oxidation of NADPH at 340 nm (ϵ_{340} 6210 $M^{-1} \cdot cm^{-1}$) with 10–100 nM enzyme and NADPH at saturating concentration (200 μM). The initial arachidonate concentration was varied by the addition of small volumes (< 2.0 μl) from the 33 mM or 3.3 mM alcoholic stock using a Hamilton syringe (Hamilton, Reno, NV, U.S.A.), and the initial laurate concentration was varied by dilution of the 1.1 mM aqueous stock. Rate measurements were converted into activity units (mol of NADPH oxidized/min per mol of P450) and plotted against fatty acid concentration, and the data were fitted to the Michaelis–Menten equation using Origin.

Stopped-flow kinetic analysis of laurate oxidation by Phe-87 mutants

The steady-state conditions for the NADPH-dependent oxidation of laurate (as described above) were set up on the stopped-flow spectrophotometer to monitor the early stage of the reaction catalysed by the F87Y and F87G mutant enzymes. The progress curves obtained with initial laurate concentrations of 50–950 μM for these reactions were fitted using the term $\{P1 \cdot [1 - e^{(-P2 \cdot t)}/P2]\} + P3 \cdot t$, which describes a deactivation process (exponential rate, P2) to a steady-state (linear) rate (P3) from an initial (short) steady-state rate (P1) over time (t) [30]. Rates P1, P2 and P3 were each plotted against laurate concentration, and the data were fitted to the Michaelis–Menten equation using Origin software.

Cytochrome *c* reduction

Initial rates of NADPH-dependent reduction of horse heart cytochrome *c* catalysed by wild-type and mutant forms of P450 BM3 were measured at 550 nm (using $\Delta\epsilon_{550} = 22640\ M^{-1} \cdot cm^{-1}$ for reduced-minus-oxidized cytochrome *c*) with 1–5 nM enzyme and 200 μM NADPH.

Flavin-to-haem electron transfer

Measurement of the rate of flavin-to-haem electron transfer was performed at 30 °C as described previously [25], using CO-saturated buffers and monitoring formation of the ferrous-iron–CO adduct at 450 nm. One syringe contained NADPH (400 μM) and laurate (930 μM), and the second syringe contained wild-type or mutant P450 BM3 (1–5 μM) and laurate (930 μM), both in assay buffer previously deoxygenated (by bubbling extensively with oxygen-free nitrogen) and saturated with CO by bubbling for 5 min. Rates were obtained by fitting the progress curves obtained to a single exponential process using the Applied Photophysics software.

H_2O_2 titration

The extent of the uncoupling of NADPH oxidation from fatty acid oxidation was assessed by titration of total H_2O_2 formed following complete oxidation of 200 μM NADPH by wild-type or mutant forms of P450 BM3, with an initial laurate concentration of 950 μM and using the *o*-dianisidine/horseradish peroxidase assay described by Macheroux et al. [31]. Following complete oxidation of NADPH (monitored at 340 nm), *o*-dianisidine was added (final concentration 8 mM) and the total increase in absorbance at 440 nm due to formation of the *o*-dianisidine radical dication oxidized product was measured after addition of horseradish peroxidase (0.1 μM). This absorbance value was converted into a concentration of *o*-dianisidine oxidized using the known coefficient ($\Delta\epsilon_{440} = 11600\ M^{-1} \cdot cm^{-1}$); this equals the H_2O_2 concentration.

RESULTS

Fatty acid binding and kinetics of fatty acid oxidation

Wild-type P450 BM3

The substrates laurate and arachidonate were used to assess the effects of active-site mutation on substrate binding and kinetic characteristics. Previous studies have shown that laurate binding to wild-type P450 BM3 induces a low- to high-spin state shift of < 30 % at saturating concentrations of laurate [21,32], that binding is characterized by a K_d of approx. 90–110 μM (e.g. [15]), and that steady-state kinetic measurements of laurate mono-oxygenation yield a k_{cat} of ≈ 1200 min^{-1} and a K_m of ≈ 100 μM at 30 °C (e.g. [33,34]). In a previous paper, we reported a k_{cat} of 1252 min^{-1} and a K_m of 89 μM for laurate mono-oxygenation, which yields a k_{cat}/K_m of 14.1 $\mu M^{-1} \cdot min^{-1}$ [34]. For these previous experiments, the sodium laurate stock solution (50 mM) was prepared in ethanol, such that kinetic measurements were performed in the presence of low (but significant) concentrations of ethanol (0.02–0.5 %, v/v). In the present study, we prepared a 1.1 mM solution of laurate in assay buffer (near the solubility limit) to permit rate measurements at laurate concentrations up to ≈ 1 mM and to eliminate the uncertainty in rate measurement brought about by the presence of organic solvent.

The induced spectral shifts on the haem Soret band of P450 BM3 in aqueous 1 mM laurate remained at ≈ 30 % (spectra not shown), but a spectrophotometric titration yielded a K_d some 2.5-fold higher (241 μM) with aqueous laurate than with the alcoholic stock. Kinetic measurements of laurate oxidation, monitored by following the initial rate of oxidation of NADPH at 340 nm and using dilutions of the 1 mM aqueous stock to obtain the Michaelis–Menten curve, yielded parameters with higher values than those obtained with the alcoholic laurate stock. The curve is characterized by a K_m of 288 μM and a k_{cat} of 5140 min^{-1} (Figure 2). It is important to note that the k_{cat}/K_m for this experiment (17.8 $\mu M^{-1} \cdot min^{-1}$) is similar to that obtained using the previous method.

The low- to high-spin shift of the haem Soret band induced upon binding of arachidonate to P450 BM3 is much larger than that for laurate (typically > 90 % conversion at a saturating concentration of arachidonate) [21], and the binding is much stronger ($K_d = 3.6$ μM). The rate of arachidonate oxidation is also much higher. In the present study, we have determined a k_{cat} of 17100 min^{-1} and a K_m of 4.7 μM, from measurements of the initial rates of arachidonate-induced NADPH oxidation. Thus the k_{cat}/K_m for this oxidation is 3640 $\mu M^{-1} \cdot min^{-1}$.

Mutants R47A and R47G

The guanidinium of Arg-47 at the mouth of the substrate-binding site (Figure 1) is thought to provide an important ion-pair interaction with the fatty acid carboxylate group [12]. Removal of this group by mutation of Arg-47 has deleterious effects on the binding and catalytic characteristics of the enzyme. For both the R47A and R47G mutants, the low- to high-spin

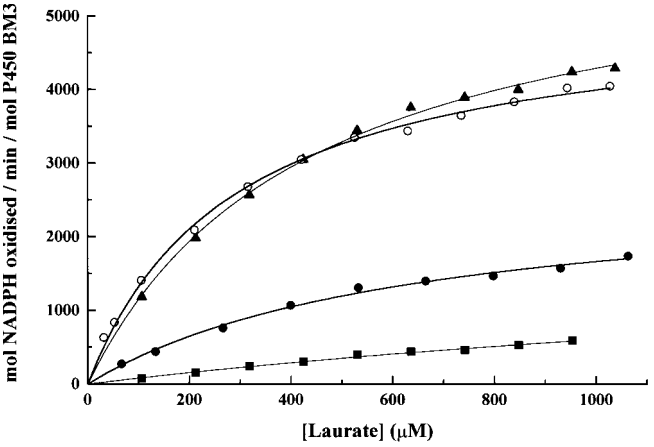

Figure 2 Michaelis–Menten curves for the NADPH-dependent oxidation of sodium laurate catalysed by wild-type flavocytochrome P450 BM3 (○) and mutants Y51F (▲), R47G (●) and F42A (■)

Initial rates were determined by monitoring the oxidation of NADPH at 340 nm at 30 °C in assay buffer, as described in the Experimental section. The data are characterized by the following parameters: wild-type P450, K_m 288 ± 15 μM, k_{cat} 5140 ± 90 min^{-1}; R47G, K_m 648 ± 50 μM, k_{cat} 2745 ± 95 min^{-1}; Y51F, K_m 432 ± 20 μM, k_{cat} 6140 ± 120 min^{-1}; F42A, K_m 2.08 ± 0.38 mM, k_{cat} 2450 ± 580 min^{-1}.

conversion induced by binding of laurate or arachidonate is considerably less than for the wild-type enzyme. The kinetic parameters (k_{cat}, K_m and k_{cat}/K_m) are presented in Table 1. There is an increase in K_m and a decrease in k_{cat} for the oxidation of laurate and arachidonate by both Arg-47 mutants as compared with the wild-type (Figure 2). The K_m and k_{cat} values for the R47A-catalysed oxidations are greater than those with the R47G mutant, but the k_{cat}/K_m values for the two mutants are similar, and demonstrate 4- and 7-fold decreases in catalytic efficiency over wild-type for the oxidation of laurate and arachidonate respectively.

Mutant Y51F

The hydroxy group of Tyr-51 has also been implicated in stabilization of the fatty acid carboxylate group via a hydrogen-bond interaction. Indeed, it has been postulated to provide a more important interaction than that of Arg-47 [12]. However, we found that removal of the hydroxy group in mutant Y51F had less detrimental effects on the catalytic parameters than those observed with the R47A/G mutants. The predominant effect is on K_m values for the oxidation of both laurate and arachidonate by Y51F (Figure 2). For laurate oxidation, the K_m is 1.5-fold greater than the wild-type value (Table 1), while there is a slight increase in k_{cat} (6140 min^{-1}). For arachidonate oxidation, K_m is 3-fold greater than wild-type, while k_{cat} is only 18 % lower (14040 min^{-1}). The effect on k_{cat}/K_m for fatty acid oxidation catalysed by Y51F is only a 1.25-fold decrease for laurate oxidation and a 3.8-fold decrease for arachidonate oxidation relative to the oxidations catalysed by the wild-type enzyme (Table 1). These data demonstrate that Tyr-51 is less important than Arg-47 in the enzyme–substrate interaction.

Mutant F42A

The phenyl group of Phe-42 lies across the mouth of the substrate-binding channel of P450 BM3 [11], and appears to act as a hydrophobic 'lid' over the active site (Figure 1). Of the three residues that we have mutated at the mouth of the active site, the most dramatic effects on substrate binding and on the catalytic parameters for substrate oxidation were observed with F42A. The low- to high-spin shift induced in the Soret band by 1 mM sodium laurate is very small (< 5 %). For the F42A-catalysed oxidation of laurate, the K_m is increased more than 7-fold over wild-type (to > 2 mM) (Figure 2). Up to the limit of solubility of sodium laurate in the assay buffer (≈ 1 mM), the increase in rate is still almost linear with concentration, and a best fit of the Michaelis–Menten equation to the data yields a k_{cat} of ≈ 2450 min^{-1}. The value of k_{cat}/K_m is 15-fold lower than that for the wild-type enzyme (Table 1). Laurate does not induce a large enough spin-state shift in F42A to enable the determination of a K_d for this substrate. Arachidonate does induce partial conversion into the high-spin form (≈ 35 % at 66 μM arachidonate), and the K_d is 19.3 ± 1.3 μM. As with laurate oxidation, there is a 7-fold increase in K_m for arachidonate oxidation by F42A, but the k_{cat} (14620 min^{-1}) is similar to the wild-type value. The k_{cat}/K_m is decreased 9-fold relative to that for wild-type (Table 1).

Cytochrome *c* reduction kinetics

To ensure that mutations made in the haem domain did not influence the electron-transfer properties of the diflavin domain, we determined the kinetic characteristics of the reduction of cytochrome *c* catalysed by wild-type and mutant P450 BM3 enzymes. Initial rates of reduction were measured with 2.0–60 μM cytochrome *c*, and the steady-state rates (mol of cytochrome *c* reduced/min per mol of P450) were plotted against cytochrome *c* concentration. There was little variation in either k_{cat} or K_m for the reduction catalysed by the mutants as compared with the wild-type (K_m within range 12.0 ± 3.0 μM; k_{cat} within range

Table 1 Kinetic parameters for oxidation of laurate and arachidonate catalysed by wild-type and mutant flavocytochromes P450 BM3

Initial-rate measurements of the oxidation of NADPH were performed at 30 °C in assay buffer (20 mM Mops/100 mM KCl, pH 7.4), as described in the Experimental section.

	Laurate oxidation			Arachidonate oxidation		
Enzyme	K_m (μM)	k_{cat} (min^{-1})	k_{cat}/K_m (μM^{-1}·min^{-1})	K_m (μM)	k_{cat} (min^{-1})	k_{cat}/K_m (μM^{-1}·min^{-1})
Wild-type	288 ± 15	5140 ± 90	17.8 ± 1.4	4.70 ± 0.25	17100 ± 190	3640 ± 245
R47A	859 ± 79	3960 ± 180	4.6 ± 0.7	18.8 ± 3.9	10640 ± 750	566 ± 198
R47G	648 ± 50	2745 ± 95	4.2 ± 0.6	9.8 ± 1.7	4855 ± 210	495 ± 130
Y51F	432 ± 20	6140 ± 120	14.2 ± 1.0	14.8 ± 1.8	14040 ± 520	949 ± 171
F42A	2080 ± 380	2450 ± 580	1.18 ± 0.6	34.9 ± 2.7	14620 ± 490	419 ± 50

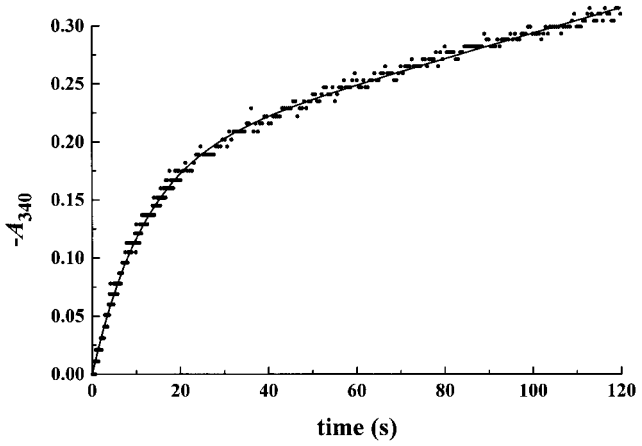

Figure 3 Progress curve for the oxidation of NADPH (at 340 nm) catalysed by the F87G mutant of P450 BM3 in the presence of sodium laurate, using stopped-flow kinetics

The reaction was followed using stopped-flow kinetics at 30 °C in assay buffer. Initial concentrations of NADPH and sodium laurate in the mixing chamber were 200 μM and 930 μM respectively, and the enzyme concentration was 0.26 μM. The form of the progress curve observed for F87G was also seen for the F87Y-mutant-catalysed reactions. The absorbance–time data collected using the stopped-flow spectrophotometer are represented as dots, and the solid line is the best fit to the term $\{P1 \cdot [1 - e^{(-P2 \cdot t)}/P2]\} + P3 \cdot t$, which describes an initial 'fast' steady state (P1) followed by a deactivation process (exponential rate; P2) to a 'slow' steady-state rate (P3) [30]. Rates P1, P2 and P3 correspond to 596 mol/min per mol, 4.0 min^{-1} and 40 mol/min per mol respectively. The kinetic parameters describing the laurate-concentration-dependence of each of these rates for the F87G and F87Y mutants are given in Table 2.

14000 ± 2000 min^{-1}) (results not shown). These small differences are likely to be attributable to some variations in the FMN content in the enzyme preparations. The FMN cofactor is essential for efficient transfer to cytochrome *c*, but is the more weakly bound flavin [35], and a small proportion will be lost during purification.

Kinetic behaviour of Phe-87 mutants

The reaction progress for the oxidation of laurate catalysed by wild-type P450 BM3 and by Arg-47, Tyr-51 and Phe-42 mutants followed true steady-state kinetics, i.e. exhibiting a linear absorbance change until substrate depletion/product accumulation became significant. However, we have noted that the steady-state kinetic behaviour of oxidation catalysed by both the F87Y and F87G mutants is unusual. Rather than observing the expected linear behaviour of the initial stage of the reaction, the reaction progress was noticeably non-linear over this period, subsequently entering a much slower linear phase. This behaviour was assessed in more detail using stopped-flow kinetics. The experimental design using the stopped-flow system was identical to that for the conventional spectrophotometric steady-state assays, i.e. monitoring the progress of the oxidation of laurate by measuring NADPH oxidation at 340 nm. The stopped-flow apparatus was set up so that reactions could be followed using a split time base, with a short initial phase (10–20 s) followed by a much longer second phase (typically > 200 s). Data were collected over a concentration range of 50–950 μM laurate. A typical reaction trace is shown in Figure 3. The form of the progress curves obtained suggested that the oxidation reactions catalysed by the F87Y and F87G mutants were characterized by an initial, short (fast) steady-state phase followed by an irreversible exponential conversion to yield a second (slower) steady-state phase. Analysis of the data using an equation describing such a process [30] (see the Experimental section) gave good fits. Plots of the two steady-state rates ('fast' and 'slow') and the conversion rate thus determined against laurate concentration showed adherence to Michaelis–Menten kinetics. The kinetic parameters characterizing both the F87Y- and F87G-catalysed reactions are shown in Table 2. These results suggest that the Phe-87 mutants undergo an irreversible conformational change during catalytic turnover which results in decreased catalytic competence.

Stopped-flow measurement of flavin-to-haem electron transfer

The rate of electron transfer from flavin to haem in fatty acid-bound P450 BM3 is conveniently measured using CO-saturated buffers and monitoring the formation of the ferrous iron–CO adduct at 450 nm using stopped-flow kinetics [25]. Binding of CO to ferrous P450 BM3 is extremely rapid ($k_{on} \sim 4 \times 10^6$ $M^{-1} \cdot s^{-1}$ at 20 °C), although binding of dioxygen may occur considerably faster [36]. We measured the rates of flavin-to-haem electron transfer at 30 °C by rapid mixing of CO-saturated solutions of (a) NADPH (400 μM) and laurate (930 μM) with (b) wild-type or mutant P450 BM3 enzymes (1–5 μM) and laurate (930 μM). The data were compared directly with the steady-state rates measured by monitoring NADPH oxidation (Table 3). The rates of flavin-to-haem transfer in all the mutants were lower than for the wild-type enzyme. Indeed, for all the mutants, the stopped-flow rate observed for the first electron transfer to the haem was decreased to a value very similar to the steady-state rate. This indicates that flavin-to-haem electron transfer is the major rate-limiting step in laurate oxidation catalysed by these mutants. For the F87Y and F87G mutants, the flavin-to-haem transfer rate corresponded to the steady-state rate of NADPH oxidation catalysed by the 'fast' form of the enzyme (Table 2). However,

Table 2 Kinetic characteristics of the oxidation of sodium laurate catalysed by F87G and F87Y mutant flavocytochromes P450 BM3

Reactions were performed at 30 °C in assay buffer. Progress curves of the oxidation of NADPH, obtained by stopped-flow kinetics at 340 nm, were fitted to the term $\{P1 \cdot [1 - e^{(-P2 \cdot t)}/P2]\} + P3 \cdot t$, which describes an initial 'fast' steady-state rate (P1) followed by a deactivation process (exponential rate; P2) to a 'slow' steady-state rate (P3) [30] (see Figure 3). Rates P1, P2 and P3 were each plotted against laurate concentration, and the data were fitted to the Michaelis–Menten equation. The term k_{conv} is the maximum rate of conversion to the 'slow' oxidizing form of F87G/Y, while K_c is the laurate concentration at $0.5 \times k_{conv}$.

	'Fast' steady state		'Slow' steady state		Conversion	
Mutant P450 BM3	K_m (μM)	k_{cat} (min^{-1})	K_m (μM)	k_{cat} (min^{-1})	K_c (μM)	k_{conv} (min^{-1})
F87G	476 ± 195	760 ± 140	290 ± 60	48.0 ± 3.7	213 ± 65	4.9 ± 0.5
F87Y	42.3 ± 9.0	1620 ± 50	84.4 ± 13.5	44.6 ± 1.4	268 ± 120	23.8 ± 3.6

Table 3 Flavin-to-haem electron transfer rates for wild-type flavocytochrome P450 BM3 and mutants, obtained by stopped-flow kinetics

Flavin-to-haem electron transfer rates were measured as a k_{obs} at 930 μM laurate. These rates are compared with the steady-state rates of NADPH oxidation at 930 μM laurate by wild-type and mutant enzymes. Stopped-flow measurements of the formation of the Fe^{2+}–CO adduct at 450 nm were performed in CO-saturated buffer containing 200 μM NADPH and 930 μM laurate at 30 °C in assay buffer, as described in the Experimental section. * Indicates that values are derived from the Michaelis–Menten curve for the 'fast' oxidizing forms of F87G and F87Y.

P450 BM3	Flavin-to-haem electron transfer rate (min^{-1})	Steady-state rate of NADPH oxidation (mol/min per mol)
Wild-type	8340 ± 50	4100 ± 150
R47A	1660 ± 20	2000 ± 90
R47G	1716 ± 20	1600 ± 85
Y51F	3740 ± 50	4000 ± 130
F42A	606 ± 5.0	650 ± 30
F87G	885 ± 30	500 ± 30*
F87Y	1600 ± 125	1480 ± 70*

in the case of the wild-type enzyme, we have measured a flavin-to-haem transfer rate that is 2-fold faster than the steady-state rate (k_{obs} 8340 min^{-1}, compared with 4100 mol/min per mol), indicating that other steps along the catalytic pathway may also limit the rate.

Determination of uncoupling in wild-type and mutant enzymes

The measurement of total H_2O_2 formed during the oxidation of all available NADPH under steady-state oxidation of laurate was carried out by direct titration using an *o*-dianisidine/horseradish peroxidase assay [31] (see the Experimental section). This is a convenient and accurate method, since it avoids the errors associated with fatty acid oxidation product recovery and quantification. Using this method, we have measured the extent of uncoupling of NADPH oxidation to be 3.8 % for the wild-type-enzyme-catalysed oxidation of laurate. For all mutants, the extent of uncoupling never exceeded 8 %, except in the case of F87Y (10 %). In the case of the Y51F-mutant-catalysed reaction, it was found that NADPH oxidation was exceptionally well coupled to laurate oxidation (only 0.16 % H_2O_2 formed).

Binding of ImC12 and 1-PIM to wild-type and mutant P450 BM3

We have described previously the potent inhibitory properties of imidazolyl fatty acids on the catalytic behaviour of P450 BM3, and their binding characteristics towards both substrate-free and substrate-saturated enzyme forms [37]. In the present study, we have measured the affinity of both ImC12 and the tight-binding 1-PIM for the wild-type enzyme and mutants Y51F, F42A, R47A/G and F87G/Y to probe the active-site environment. The nitrogen atom of the imidazole moieties of ImC12 and 1-PIM ligates to the ferric haem, causing a type II shift in the Soret band from 419 to 424 nm (Figure 4), but the affinity of the interaction is modulated by the surrounding active-site structure. K_d values were determined by plotting these induced spectral changes against imidazole concentration, as described in the Experimental section (Table 4). Binding of ImC12 to wild-type P450 BM3 is characterized by a K_d of 8.0 μM. Binding is much weaker to the Arg-47 mutants (e.g. K_d 42.2 μM for R47G), due to removal of the interaction between the fatty acid carboxylate group and the guanidinium group of Arg-47. Remarkably, the affinity of ImC12 for Y51F is considerably stronger than that for the wild-type enzyme (K_d 0.22 μM). This could be due to loss of a hydrogen bond between the hydroxy group of Tyr-51 and the guanidinium group of Arg-47, resulting in an increase in cationic charge on Arg-47 available for interaction with the carboxy group of ImC12. The removal of the phenyl group of Phe-42 also has the effect of increasing the affinity for ImC12 (K_d 2.5 μM for F42A). This may be due to an increased accessibility to the haem for this inhibitor. The tighter binding of ImC12 to mutants Y51F and F42A relative to the wild-type enzyme contrasts with the catalytic situation, where the K_m values for these two mutants with laurate are increased ($\approx$ 1.5-fold for Y51F, but $>$ 7-fold in the case of F42A). K_d values for the binding of laurate to mutants Y51F and F42A cannot be determined spectrophotometrically, because

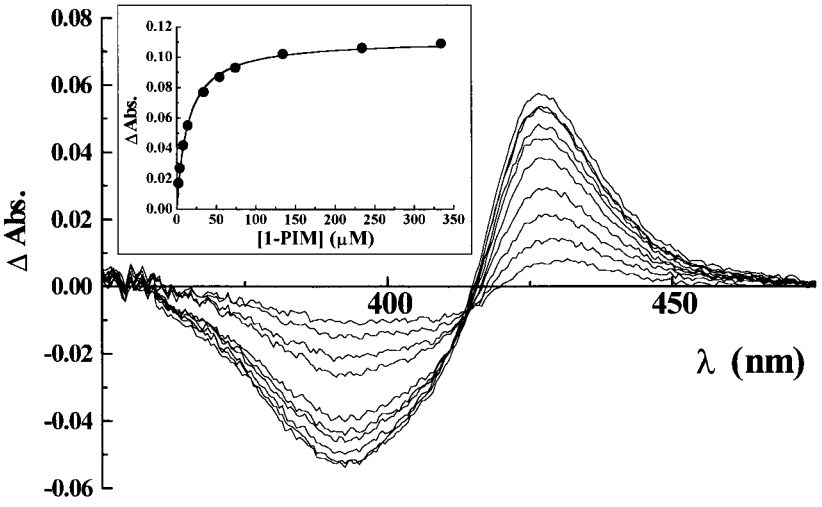

Figure 4 Absorbance difference spectra recorded during the titration of wild-type P450 BM3 (2 μM) with 1-PIM (2–334 μM)

The binding of 1-PIM results in a shift of the Soret band of the P450 from 419 nm to 424 nm in the absolute spectrum. In the difference spectra, the maximal absorbance changes (ΔAbs.) induced at each concentration of 1-PIM [absorbance change at 427 nm (ΔA_{427}) − absorbance change at 393 nm (ΔA_{393})] are plotted against 1-PIM concentration, and the data are fitted to the Michaelis function (inset), as described in the Experimental section. This yields the K_d for binding of the ligand (10.4 μM in this case).

Table 4 Dissociation constants for the binding of ImC12 and 1-PIM to wild-type and mutant flavocytochromes P450 BM3

Titrations were performed spectrophotometrically at 30 °C in assay buffer. Details of the experimental design and the treatment of the spectral data to obtain the K_d values are given in the Experimental section. *Indicates that the titration was performed using a 5 cm path-length cuvette.

	K_d (μM)	
P450 BM3	ImC12	1-PIM
Wild-type	8.0 ± 0.2	10.4 ± 0.4
R47A	35.4 ± 1.2	4.2 ± 0.1
R47G	42.2 ± 1.0	6.7 ± 0.3
Y51F	0.22 ± 0.01*	8.3 ± 0.6
F42A	2.5 ± 0.2	7.3 ± 0.2
F87G	5.3 ± 0.1	0.8 ± 0.03
F87Y	24.3 ± 2.6	7.1 ± 1.1

the spin-state shifts observed in the Soret bands are too small. However, we have been able to determine K_d values for binding of arachidonate to the F42A and Y51F mutants, since the spectral changes accompanying binding are much larger. Binding of arachidonate to F42A mutant P450 BM3 is characterized by a K_d of 19.3 ± 1.3 μM, considerably weaker than binding to wild-type (K_d 3.6 μM). By contrast, binding of arachidonate to the Y51F mutant is tighter (K_d 0.68 μM), although the extent of the induced spin-state shift as a result of this binding ($\sim 50\%$) is not as great as in the wild-type enzyme ($> 90\%$).

Binding of 1-PIM to wild-type P450 BM3 is characterized by a K_d of 10.4 μM, i.e. weaker than the binding to the mutant forms (Table 4). Mutants R47A, R47G, Y51F and F42A all display slightly increased affinities towards 1-PIM (K_d values in the range 4.2–8.3 μM), presumably due to improved accessibility to the haem. The most notable effect on binding is observed with the F87G mutant, where the affinity is increased 13-fold over wild-type (K_d 0.8 μM). The removal of the Phe-87 phenyl group may leave a hydrophobic space in which the phenyl group of 1-PIM can bind efficiently, explaining the very tight ligation of 1-PIM to this mutant.

DISCUSSION

In this study, we have determined the kinetic consequences of the mutation of important active-site residues in flavocytochrome P450 BM3. In particular, we have resolved the relative contributions of the side chains of Arg-47 and Tyr-51 to fatty acid binding and catalysis. This pair of residues forms a hydroxy–guanidinium interaction at the mouth of the fatty-acid-binding channel, and both associate with the carboxy group of the fatty acid substrate. The decreases in k_{cat} and increases in K_m for the oxidation of laurate and arachidonate catalysed by the R47A and R47G mutant enzymes relative to wild-type demonstrates that the electrostatic interaction between the Arg-47 guanidinium group and the fatty acid carboxy group is involved in both initial binding and transition-state stabilization. In contrast, for the Y51F-mutant-catalysed oxidations, the K_m is increased but k_{cat} is essentially unaffected, showing that the hydrogen-bonding interaction between the hydroxy group of Tyr-51 and the fatty acid carboxy group is important only for initial binding. It should be emphasized that contributions other than those from Arg-47 and Tyr-51 are important to the binding of fatty acids in the P450 BM3 active site. Indeed, if the ion-pair interaction between Arg-47 and the fatty acid carboxylate was the main stabilizing factor in the binding of fatty acid substrate, then much larger increases in the K_m and K_d values for fatty acid substrates would be expected with the mutants [38]. However, other favourable interactions occur between the fatty acid alkyl chain and multiple hydrophobic amino acids (such as Leu-181 and Leu-437) in the long channel leading down from Arg-47/Tyr-51 to the haem. The major purpose of the interactions between the fatty acid carboxylate group and Arg-47/Tyr-51 is likely to be in the correct positioning of substrate to promote efficient active-site dehydration and the accompanying haem iron spin-state conversion which is critical for catalysis [21].

The presence of both a positively charged amino acid and a hydroxy-group-containing amino acid (Arg-47 and Tyr-51 in P450 BM3) interacting with the carboxylate of a substrate molecule is an active-site motif that is conserved in certain other enzymes, and the catalytic effects (increased K_m, but similar k_{cat}) of the removal of the hydroxy moiety of this pairing are similar to those that we have observed in P450 BM3. For example, the tetrameric L-lactate cytochrome *c* oxidoreductase (flavocytochrome b_2) from *Saccharomyces cerevisiae* uses Arg-376 and Tyr-143 to stabilize the binding of lactate. The flavocytochrome b_2 mutant Y143F shows a 6-fold increased K_m and an unchanged k_{cat} relative to wild-type using L-lactate as a substrate and ferricyanide as the electron acceptor [39,40]. The motif is also conserved in flavocytochrome b_2 from *Hansenula anomala* (Arg-362 and Tyr-135) [41] and in the closely related *Rhodotorula graminis* L-mandelate dehydrogenase (Tyr-25 and Arg-277), which is also a tetrameric flavocytochrome [42]. Similarly, mutation Tyr-24 → Phe in spinach glycolate oxidase (containing Tyr-24 and Arg-257 in the active site) results in a 10-fold increased K_m and an unchanged k_{cat} for glycolate oxidation [43]. In *Bacillus stearothermophilus* lactate dehydrogenase, a serine residue (Ser-163) replaces tyrosine in hydrogen-bonding to the the lactate, but the hydroxy amino acid motif is retained [44]. In this enzyme, Arg-171 is the analogue of Arg-47 in P450 BM3. Mutant R171K of the lactate dehydrogenase exhibits much higher K_m and lower k_{cat} values than the wild-type enzyme [45]. Again, this is similar to the effects that we observed on the catalytic parameters of the R47G/A mutants of P450 BM3 [45].

The spin-state shifts induced by the binding of arachidonate to the R47G and Y51F mutants of P450 BM3 are sufficient to allow determination of K_d values: R47G, K_d 7.1 μM, spin-shift $\approx 20\%$; Y51F, K_d 0.68 μM, spin-shift $\approx 35\%$. Arachidonate binding to the wild-type enzyme is characterized by a K_d of 3.6 μM and results in a $> 90\%$ spin-state shift. Hence the affinity of arachidonate for the Y51F mutant appears to be higher than that for the wild-type, while that for the R47G mutant is lower. It is very interesting to note that the K_d values for fatty acid substrate and imidazole-linked fatty acid (ImC12) binding to Y51F are decreased relative to wild-type, whereas the K_m values for Y51F-catalysed substrate oxidation are increased (Tables 1 and 4). Most notable is the huge (30-fold) increase in the affinity of the Y51F mutant for ImC12. For the R47A/G and Y51F mutants, the extent of the low-to-high spin-state shift induced by binding of fatty acid is considerably lower than for the wild-type enzyme. Despite the higher affinity for Y51F, the binding mode adopted by the fatty acid does not result in efficient active-site desolvation, and the Y51F haem iron population remains substantially low-spin, i.e. with the aqua (6th) ligand still present. These results demonstrate that the interaction between the fatty acid carboxy group and the hydroxy group of Tyr-51 is essential to induce the efficient low-to-high spin-state shift required for elevation of the haem reduction potential [21]. We postulate that the absence of the hydroxy group of Tyr-51

has the effect of strengthening the electrostatic interaction between the guanidinium of Arg-47 and the carboxylate group of the substrate, resulting in higher apparent affinity, but also in a different binding mode from which the 6th (aqua) haem ligand cannot be displaced efficiently. The observation that trends in K_d values for substrate/inhibitor binding do not reflect the trends in K_m values for substrate oxidation emphasizes the point that the K_d is purely a single equilibrium binding constant determined by spectrophotometric titration of the oxidized enzymes, whereas the K_m (determined under steady-state turnover conditions) is a complex term comprising multiple binding constants throughout the catalytic pathway.

In the structure of the substrate-free P450 BM3 haem domain [11], the phenyl side chain of Phe-42 lies close to the mouth of the active site at the protein surface. However, in the substrate-bound form the side chain is repositioned and 'caps' the mouth of the binding site, effectively protecting the substrate in its hydrophobic environment and probably also strengthening the electrostatic interaction between the substrate carboxy group and the guanidinium group of Arg-47 by excluding solvent water. The catalytic effects of mutation of this residue are dramatic. The predominant effect is on K_m. For the F42A-catalysed oxidations of both laurate and arachidonate, the K_m is increased $>$ 7-fold over that with the wild-type enzyme, whereas the k_{cat} is decreased 2-fold (laurate) and 1.2-fold (arachidonate). There is a consequent large decrease in k_{cat}/K_m (15- and 9-fold for laurate and arachidonate respectively). We believe that the F42A mutation leaves the active site more exposed to solvent, resulting in considerable weakening of the guanidinium–carboxy interaction. However, such large effects on catalytic parameters are not observed for Arg-47-mutant-catalysed fatty acid oxidations, for which the guanidinium–carboxy interaction is absent. This suggests that the F42A mutation has other consequences. The phenyl group of Phe-42 may form a key part of the hydrophobic surface, which also comprises residues Phe-11, Leu-14, Leu-17, Pro-18 and Leu-19, and which has been suggested to be a fatty acid recognition/docking region [11,46]. Both the increased access of water and the absence of a substrate-recognition amino acid would be expected to have effects on K_m. However, the absence of the phenyl 'cap' allows easier access of ImC12 to the active-site pocket, which is reflected in the 3-fold decrease in the K_d for this inhibitor (Table 4).

The structures of the substrate-free and -bound forms of P450 BM3 show that large conformational changes occur on substrate binding, with a narrowing of the binding pocket around the substrate and considerable re-orientation of several active-site side chains [12]. One such side-chain motion involves the phenyl group of Phe-87, which rotates from a conformation almost perpendicular to the haem plane in the substrate-free form to lie parallel when substrate is bound. NMR paramagnetic relaxation studies have shown that, upon reduction of the ferric iron, the substrate moves some 6 Å (0.6 nm) closer to the haem [47]. This movement must be accompanied by further conformational changes also involving Phe-87, but the nature of these changes is unknown. Phe-87 is known to control the regiospecificity of fatty acid oxidation. Oliver et al. [23] reported that mutant F87A hydroxylates laurate at the terminal (ω) position, whereas wild-type P450 BM3 hydroxylates mainly at $\omega-2$. The mutant retains good laurate oxidation activity, indicating that substitution of the phenyl ring for a methyl group retains sufficient hydrophobicity to allow interaction with the terminal part of the alkyl chain of the fatty acid. We have shown that the rates of laurate oxidation catalysed by both the F87G and F87Y mutants are considerably lower than that with the wild-type enzyme. For F87G, this may be due to the absence of favourable hydrophobic binding interactions with the terminus of the alkyl chain, while for F87Y such interactions could be disrupted by the presence of the tyrosine hydroxy group. Crucially, Phe-87 also appears to be instrumental in facile conformational switching of the enzyme during the catalytic cycle. Our results suggest that both the F87Y and F87G mutants undergo an irreversible deactivation process during catalysis of laurate oxidation, from an initial 'fast' oxidizing form, through an exponential conversion into a 'slow' oxidizing form. We can propose two possibilities to explain this behaviour. First, there may be an irreversible conformational change during turnover. Alternatively, there may be a change in the rate-limiting step, either to a conformational-switching limit or to a product-release limit. In wild-type- and Arg-47/Tyr-51/Phe-42-mutant-catalysed reactions, conformational switching is rapid. Immediately after its formation, the oxidation product must still be protected within the active site, and rapid conformational changes occur which cause it to be released. The first flavin-to-haem electron transfer is observable as the main determinant of the overall rate (as demonstrated by the stopped-flow kinetic studies of flavin-to-haem electron transfer). However, for the F87G- and F87Y-mutant-catalysed reactions, we postulate that the rapid conformational switching mechanism leading to product release is disrupted. The product is held by a relatively long-lived conformer of the enzyme that exists towards the end of the catalytic cycle, so that its release (or the conformational readjustment to regain resting enzyme) is rate-limiting. By such a process, the slow reaction phase (Figure 3) retains linear steady-state characteristics over the time course we have measured. The concentration of oxidized product in the bulk solvent over this time period is too low to have a competitive inhibitory effect on the steady state, and so we do not observe a progressively decreasing rate.

In conclusion, the present studies have elucidated the roles of four important active-site residues in flavocytochrome P450 BM3. Residue Tyr-51 was postulated to provide the dominant contribution in binding the fatty acid carboxylate group [12], but our studies indicate that Arg-47 provides a stronger stabilizing interaction. However, the interaction between the fatty acid and Tyr-51 appears to be important for substrate-induced haem iron spin-state shift, which is critical to catalysis [21]. In addition to controlling the regioselectivity of substrate oxidation [23], we have identified a key role for Phe-87 in the conformational switches that occur during the catalytic cycle of P450 BM3 [12,47]. Mutants F87G and F87Y both undergo conversion into a low-activity form during turnover. We postulate that this is due to an alteration in the rate-limiting step in catalysis from a flavin-to-haem electron transfer step to product release, as a consequence of these mutations. We are currently investigating this phenomenon further. The most severe effects on catalytic efficiency are observed in mutant F42A, due to the removal of the phenyl 'cap' from the top of the active site. The mutants F42A/Y51F and F87G bind the fatty-acid-linked azole ImC12 and the smaller inhibitor 1-PIM respectively much more tightly than does wild-type P450 BM3, indicating that considerable reorganization of the active site is induced by these mutations. We are currently performing crystallographic trials with the mutant haem domains and investigating further the substrate preferences of these mutants in order to define the nature of these structural changes and their consequences.

We thank the Royal Society of Edinburgh and Caledonian Research Foundation for the awards of a Research Fellowship (A.W.M.) and an SOEID Support Fellowship (S.K.C.). We also thank the Leverhulme Trust (funding of M.A.N. and C.S.M.) and the BBSRC for continuing support for these studies. Imidazolyl fatty acids were provided by Ms. Ping Lu (Department of Medicinal Chemistry, University of Kansas).

REFERENCES

1 Lewis, D. F. V. (1996) in Cytochromes P450: Structure, Function and Mechanism, pp. 115–167, Taylor and Francis, London
2 Munro, A. W. and Lindsay, J. G. (1996) Mol. Microbiol. **20**, 1115–1125
3 Nelson, D. R., Kamataki, T., Waxman, D. J., Guengerich, F. P., Estabrook, R. W., Feyereisen, R., Gonzalez, F. J., Coon, M. J., Gunsalus, I. C., Gotoh, O. et al. (1993) DNA Cell. Biol. **12**, 1–51
4 Capdevila, J. H., Falck, J. R. and Estabrook, R. W. (1992) FASEB J. **6**, 731–736
5 Guengerich, F. P. and Shimada, T. (1991) Chem. Res. Toxicol. **4**, 391–407
6 Cole, S. T., Brosch, R., Parkhill, T., Garnier, T., Churcher, C., Harris, D., Gordon, S. V., Eiglmeier, K., Gas, S., Barry, C. E. et al. (1998) Nature (London) **391**, 537–544
7 Karlson, U., Dwyer, D. F., Hooper, S. W., Moore, E. R. B., Timmis, K. N. and Eltis, L. D. (1993) J. Bacteriol. **175**, 1467–1474
8 Nagy, I., Schloofs, G., Compernolle, F., Proost, P., Vanderleyn, J. and De Mot, R. (1995) J. Bacteriol. **177**, 676–687
9 Park, S. Y., Shimizu, H., Adachi, S., Nakagawa, A., Izuka, T. and Shiro, Y. (1997) Nat. Struct. Biol. **4**, 827–832
10 Watanabe, I., Nara, F. and Serizawa, N. (1995) Gene **163**, 81–85
11 Ravichandran, K. G., Boddupalli, S. S., Hasemann, C. A., Peterson, J. A. and Deisenhofer, J. (1993) Science **261**, 731–736
12 Li, H.-Y. and Poulos, T. L. (1997) Nat. Struct. Biol. **4**, 140–146
13 Mueller, E. J., Loida, P. J. and Sligar, S. G. (1995) in Cytochrome P450: Structure, Mechanism and Biochemistry (Ortiz de Montellano, P. R., ed.), pp. 83–124, Plenum Press, New York
14 Oliver, C. F., Modi, S., Sutcliffe, M. J., Primrose, W. U., Lian, L. Y. and Roberts, G. C. K. (1997) Biochem. J. **327**, 537–544
15 Munro, A. W., Malarkey, K., Lindsay, J. G., Coggins, J. R., Price, N. C., Kelly, S. M., McKnight, J., Thomson, A. J. and Miles, J. S. (1994) Biochem. J. **303**, 423–428
16 Imai, M., Shimada, H., Watanabe, Y., Matsushima-Hibiya, Y., Makino, R., Koga, H., Horiuchi, T. and Ishimura, Y. (1989) Proc. Natl. Acad. Sci. U.S.A. **86**, 7823–7827
17 Nelson, D. R. (1995) in Cytochrome P450: Structure, Mechanism and Biochemistry (Ortiz de Montellano, P. R., ed.), pp. 575–606, Plenum Press, New York
18 Narhi, L.-O. and Fulco, A. J. (1987) J. Biol. Chem. **262**, 6863–6870
19 Miles, J. S., Munro, A. W., Rospendowski, B. N., Smith, W. E., McKnight, J. and Thomson, A. J. (1992) Biochem. J. **288**, 503–509
20 Marletta, M. A. (1993) J. Biol. Chem. **268**, 12231–12234
21 Daff, S. N., Chapman, S. K., Turner, K. L., Holt, R. A., Govindaraj, S., Poulos, T. L. and Munro, A. W. (1997) Biochemistry **36**, 13816–13823
22 Graham-Lorence, S., Truan, G., Peterson, J. A., Falck, J. R., Wei, S. Z., Helvig, C. and Capdevila, J. H. (1997) J. Biol. Chem. **272**, 1127–1135
23 Oliver, C. F., Modi, S., Sutcliffe, M. J., Primrose, W. U., Lian, L. Y. and Roberts, G. C. K. (1997) Biochemistry **36**, 1567–1572
24 Lu, P., Alterman, M. A., Chaurasia, C. S., Bambal, R. B. and Hanzlik, R. P. (1997) Arch. Biochem. Biophys. **337**, 1–7
25 Munro, A. W., Daff, S., Coggins, J. R., Lindsay, J. G. and Chapman, S. K. (1996) Eur. J. Biochem. **239**, 403–409
26 Kunkel, T. A. (1985) Proc. Natl. Acad. Sci. U.S.A. **82**, 488–492
27 Zoller, M. J. and Smith, M. (1983) Methods Enzymol. **100**, 468–500
28 Vieira, J. and Messing, J. (1987) Methods Enzymol. **153**, 3–11
29 Okita, R. T., Vlark, J. E., Rice Okita, J. and Masters, B. S. S. (1991) Methods Enzymol. **206**, 432–441
30 Tew, D. G. (1993) Biochemistry **32**, 10209–10215
31 Macheroux, P., Massey, V., Thiel, D. J. and Volokita, M. (1991) Biochemistry **30**, 4612–4619
32 Modi, S., Primrose, W. U., Boyle, J. M. B., Gibson, C. F. and Roberts, G. C. K. (1995) Biochemistry **34**, 8982–8988
33 Narhi, L.-O. and Fulco, A. J. (1986) J. Biol. Chem. **261**, 7160–7169
34 Munro, A. W., Lindsay, J. G., Coggins, J. R., Kelly, S. M. and Price, N. C. (1994) FEBS Lett. **343**, 70–74
35 Munro, A. W., Lindsay, J. G., Coggins, J. R., Kelly, S. M. and Price, N. C. (1996) Biochim. Biophys. Acta **1296**, 127–137
36 Sevrioukova, I. F., Schaffer, C., Ballou, D. P. and Peterson, J. A. (1996) Biochemistry **35**, 7058–7068
37 Noble, M. A., Turner, K. L., Chapman, S. K., Hanzlik, R. P. and Munro, A. W. (1998) Biochemistry **37**, 15799–15807
38 Fersht, A. (1985) in Enzyme Structure and Mechanism, 2nd edn., pp. 47–97 and pp. 293–346, W. H. Freeman and Co., New York
39 Xia, Z.-X. and Mathews, F. S. (1990) J. Mol. Biol. **212**, 837–863
40 Miles, C. S., Rouviere-Fourmy, N., Lederer, F., Mathhews, F. S., Reid, G. A., Black, M. T. and Chapman, S. K. (1992) Biochem. J. **285**, 187–192
41 Black, M. T., Gunn, F. J., Chapman, S. K. and Reid, G. A. (1989) Biochem. J. **263**, 973–976
42 Smekal, O., Yasin, M., Fewson, C. A., Reid, G. A. and Chapman, S. K. (1993) Biochem. J. **290**, 103–107
43 Stenberg, K., Clausen, T., Lindqvist, Y. and Macheroux, P. (1995) Eur. J. Biochem. **228**, 408–416
44 Barstow, D. A., Clarke, A. R., Chia, W. N., Wigley, D., Sharman, A. F., Holbrook, J. J., Atkinson, T. and Minton, N. P. (1986) Gene **46**, 47–55
45 Hart, K. W., Clarke, A. R., Wigley, D. B., Waldman, A. D. B., Chia, W. N., Barstow, D. A., Atkinson, T., Jones, J. B. and Holbrook, J. J. (1987) Biochim. Biophys. Acta **914**, 294–298
46 Maves, S. A., Yeom, H., McLean, M. A. and Sligar, S. S. (1997) FEBS Lett. **414**, 213–218
47 Modi, S., Sutcliffe, M. J., Primrose, W. U., Lian, L. Y. and Roberts, G. C. K. (1996) Nat. Struct. Biol. **3**, 414–417

Received 24 August 1998/4 January 1999; accepted 29 January 1999